



CHORUS

This is the accepted manuscript made available via CHORUS. The article has been published as:

Visualizing superconductivity in FeSe nanoflakes on SrTiO₃ by scanning tunneling microscopy

Zhi Li, Jun-Ping Peng, Hui-Min Zhang, Can-Li Song, Shuai-Hua Ji, Lili Wang, Ke He, Xi Chen, Qi-Kun Xue, and Xu-Cun Ma

Phys. Rev. B **91**, 060509 — Published 27 February 2015

DOI: [10.1103/PhysRevB.91.060509](https://doi.org/10.1103/PhysRevB.91.060509)

Visualizing the superconductivity in FeSe nanoflakes on SrTiO₃ by scanning tunneling microscope

Zhi Li,¹ Jun-Ping Peng,¹ Hui-Min Zhang,¹ Can-Li Song,^{2,3,*} Shuai-Hua Ji,^{2,3}
Lili Wang,^{2,3} Ke He,^{2,3} Xi Chen,^{2,3} Qi-Kun Xue,^{2,3} and Xu-Cun Ma^{1,2,3,†}

¹*State Key Laboratory for Surface Physics, Institute of Physics,
Chinese Academy of Sciences, Beijing 100190, China*

²*State Key Laboratory of Low-Dimensional Quantum Physics,
Department of Physics, Tsinghua University, Beijing 100084, China*

³*Collaborative Innovation Center of Quantum Matter, Beijing 100084, China*

(Dated: January 26, 2015)

Scanning tunneling microscopy and spectroscopy have been employed to investigate the superconductivity in single unit-cell FeSe nanoflakes on SrTiO₃ substrate. We find that the differential conductance dI/dV spectra are spatially nonuniform and fluctuates within the flakes as their area is reduced to below ~ 150 nm². An enhancement in the superconductivity-related gap size as large as 25% is observed. The superconductivity behavior disappears when the FeSe nanoflakes reduces to ~ 40 nm². Compared to previous report [Q. Y. Wang *et al.*, Chin. Phys. Lett. 29, 037402 (2012)], the gap is asymmetric relative to the Fermi energy E_F . All the features, particularly the fluctuating gap and quenched superconductivity, could be accounted for by quantum size effects. Our study helps understand the nanoscale superconductivity in low-dimensional systems.

PACS numbers: 68.37.Ef, 74.70.Xa, 74.55.+v, 74.78.-w

I. INTRODUCTION

Superconductivity in reduced dimensions, including ultrathin films,¹⁻³ nanowires⁴ and nanograins,⁵⁻¹⁰ has still been a hot topic of interest due to its potential for developing dissipationless nanoelectronics. However, as the size of a superconductor is shrunk to nanoscale, quantum size effects (QSE) would become important and can dramatically change its superconducting properties. Many fascinating phenomena, such as the parity effect and shell effect on gap magnitude Δ , have been predicted theoretically¹¹⁻¹³ and ascertained experimentally in several conventional BCS-type superconductors.^{5-8,10} Superconductivity can be eventually quenched if the nanograin size is small enough so that the QSE induced discrete energy level spacing ($\sim 2\pi^2\hbar^2/(mk_FV)$) exceeds the bulk gap magnitude Δ_0 , where \hbar , m , k_F and V denote the reduced Planck constant, the mass of an electron, the Fermi wave vector and nanograin volume, respectively. In order to study these phenomena, nanostructures with extremely small k_FV are particularly interesting. Compared to conventional metal superconductors,^{1-8,10} the layered superconducting compounds (e.g. cuprates and iron-based superconductors) generally exhibit a smaller k_F and represent ideal systems to test the intriguing superconductivity in confined systems. However, the fabrication of small layered superconductors yet remains a great experimental challenge.

The recently discovered single unit-cell (UC) FeSe/SrTiO₃ films, with the simple crystal structure and a high transition temperature T_c ,¹⁴⁻¹⁶ has sparked considerable research efforts aimed at uncovering the electron pairing mechanism in high- T_c superconductors, such as extensive angle-resolved photoemission spectroscopy,¹⁷⁻¹⁹ theoretical^{20,21} and even *in*

situ transport studies.²² Meanwhile, the system provides a new platform for exploring QSE on unconventional superconductivity, given that the electron confinement has already been reached along the z direction. A recent theoretical work has also predicted the QSE induced T_c enhancement in iron-based superconductors.²³ So far, the T_c enhancement has been observed in FeSe encapsulated in carbonaceous shell, which was ascribed as the FeSe lattice compression effect,^{24,25} rather than QSE.

In this study, we report on scanning tunneling microscopy (STM) and spectroscopy (STS) studies of single UC FeSe nanoflakes on SrTiO₃ substrate grown by molecular beam epitaxy (MBE). The technique allows for a direct probing of the superconducting order parameter and a study of its relationship with lateral QSE. We find that (i) the gap magnitude Δ fluctuates with flake area A with a maximum value of 25 meV, larger than the previously reported value of 20.1 meV,¹⁴ (ii) the superconductivity completely disappears as the nanoflake size A is reduced below ~ 40 nm², (iii) the gap exhibits great asymmetry with respect to the Fermi energy E_F . We show that the observations are intimately correlated with the lateral QSE in FeSe nanoflakes.

II. EXPERIMENT

Our experiments were performed on an ultra-high vacuum low temperature STM (Unisoku) system with a base pressure of 5×10^{-11} Torr, which is connected to a MBE chamber for *in-situ* sample preparation. Nb-doped (0.5 wt%) SrTiO₃ was etched by Se molecular flux and then used as substrate for single UC FeSe film growth.¹⁴ The MBE growth of FeSe films has been described in detail

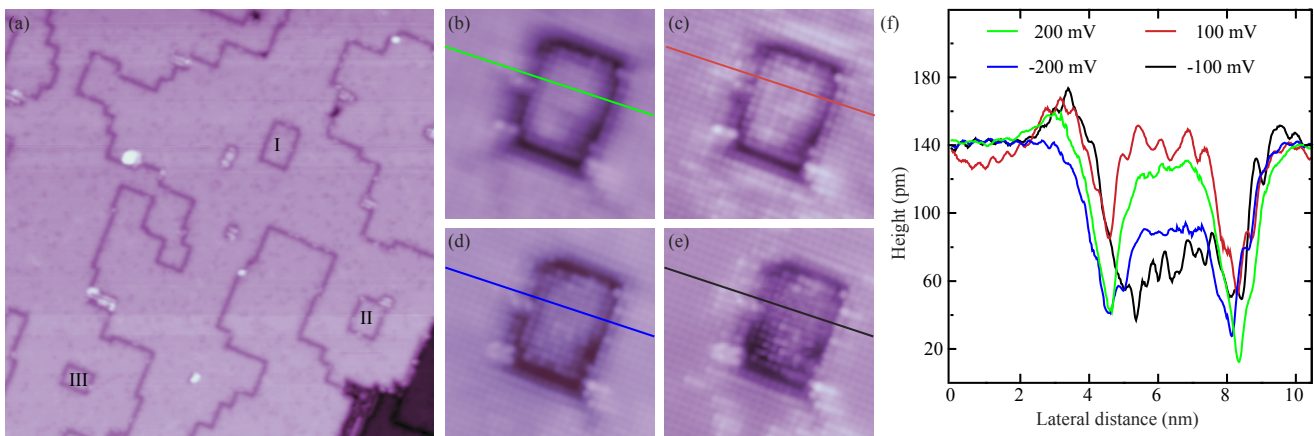


FIG. 1. (Color online) (a) STM topographic image ($V_s = 4$ V, $I = 20$ pA, 100 nm \times 100) of single UC FeSe films grown on SrTiO₃ substrate. The dark trenches are primarily caused by missing atoms. (b-e) STM topographies ($I = 30$ pA, 10 nm \times 10) in the vicinity of an isolated rectangular FeSe nanoflake, and (f) Cross-section height profiles along the straight lines in (b-e) at different sample voltages V_s . The bright spots in (b-e) correspond to the topmost Se atoms.

elsewhere.²⁶ Prior to STM/STS measurements at 4.5 K, a polycrystalline PtIr tip was first cleaned by electron-beam heating in the MBE chamber, and then calibrated with Ag/Si(111) films. Unless otherwise noted, tunneling spectra were acquired by disrupting the feedback circuit at setpoint voltage $V_s = 50$ mV and $I = 50$ pA, sweeping the sample voltage V_s , and extracting the differential tunneling conductance dI/dV using a standard lock-in technique with a small bias modulation of 0.1 mV at 987.5 Hz.

III. RESULTS AND DISCUSSIONS

Figure 1(a) depicts a typical single UC FeSe film grown on SrTiO₃ substrate. The dark trenches divide the films into many domains, as already interpreted before.²⁷ Occasionally, certain trenches connect together and can completely isolate some rectangular nanoflakes (marked by I, II and III) from the remaining FeSe films. The rectangular flakes vary from several tens to several hundreds of nm² in area. Our careful inspection reveals that the FeSe nanoflakes differ from the continuous films in their electronic structure, as illustrated in Figs. 1(b-f). The apparent height of the nanoflakes usually exhibits lower value, especially at small and negative (filled states) sample voltage V_s (for example, see Fig. 1(f)). This suggests that the FeSe nanoflakes are electronically isolated from the other regions, which enables us to detect experimentally their superconductivity. In other words, the isolated FeSe nanoflakes can serve as an ideal system for studying the interplay between lateral QSE and superconductivity.

We below focus on the dependence of the superconductivity on the nanoflake area A . Figure 2(a) shows a typical superconducting gap taken on a larger FeSe nanoflake ($A > 900$ nm²), where two E_F -symmetric superconducting coherence peaks at $\sim \pm 16.5$ meV are

clearly evident. It is worth noting that these spectra are spatially uniform over different regions of the flake, which resembles those previously reported on FeSe films in a prominent manner.¹⁶ The gap magnitude of ~ 16.5 meV, most frequently observed, is quite in line with previous measurements.^{16–19} As A is reduced, however, the spectra gradually become site-dependent, as shown in Fig. 2(b). Two intriguing features are immediately discernable. One is that Δ becomes spatially inhomogeneous and exhibits a maximum value of ~ 25 meV (black curves

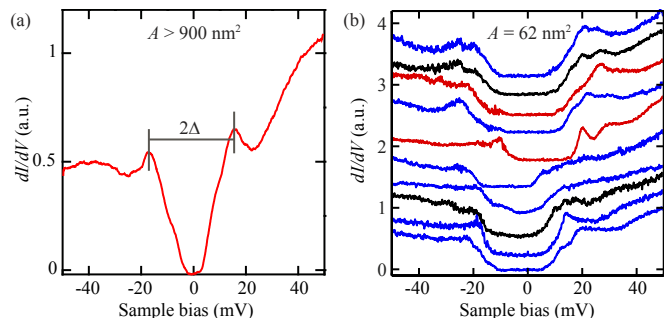


FIG. 2. (Color online) Comparison of dI/dV spectra acquired on single UC FeSe nanoflakes with different area A . (a) Typical differential conductance dI/dV spectrum in a large FeSe nanoflake ($A > 900$ nm²). Two vertical gray lines indicate the energy positions of superconducting coherence peaks, with their separation defined as 2Δ . Tunneling gap is stabilized at $V_s = 50$ mV and $I = 95$ pA. (b) Normalized dI/dV spectra taken at equal separations (~ 0.8 nm) along a line of FeSe nanoflake with $A = 62$ nm². Colored curves indicate the asymmetry of dI/dV spectra at various positions, signaling great spatial inhomogeneity. Here, we calculate 2Δ from the two strongest coherence peaks below and above E_F (not marked), respectively, in line with (a). The fine structures beyond the gaps may originate from QSE-resulted discrete energy levels.

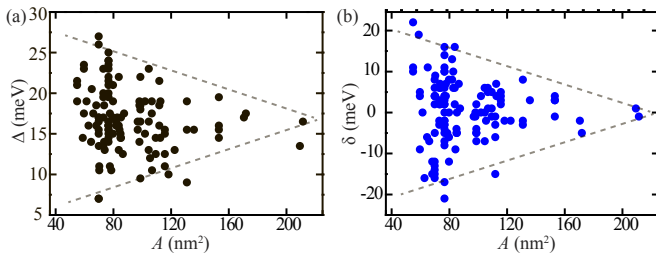


FIG. 3. (Color online) (a) Plot of gap magnitude Δ , and (b) gap asymmetry $\delta = \Delta_+ - \Delta_-$ versus FeSe nanoflake area A , with Δ_+ and Δ_- indicating the deviations of the two coherence peaks above and below E_F from E_F , respectively. Gray dotted lines are guides to eye.

in Fig. 2(b)), 25% larger than 20 meV reported previously in continuous films. The other is that the two coherence peaks appears asymmetric for most of the positions studied: they can either be positively (red curves in Fig. 2(b)) or negatively (blue curves in Fig. 2(b)) shifted in energy with respect to E_F .

Figure 3 summarizes the gap magnitude Δ and asymmetry δ for various positions and also for FeSe nanoflakes with varying A . The variation of both Δ and δ are found to be closely correlated or to fluctuate with A . A smaller flake usually leads to stronger variations in Δ and δ . These are reminiscent of the well-known shell effect in clean superconducting nanoparticles, such as Sn,¹⁰ which originates primarily from the discretization of the energy levels due to QSE in small superconducting nanoparticles. In single UC films of FeSe on SrTiO₃, the recent ARPES measurements have revealed a relatively small Fermi wavevector $k_F \sim 0.2\pi/a$ for the electron pockets around M ($a = 0.38$ nm).^{17–19} This leads to a Fermi wavelength of $\lambda_F \sim 3.8$ nm and $k_F A^{0.5} \gg 1$, since A ranges from tens to hundreds of nm² in the FeSe nanoflakes investigated here. Compared to Sn,¹⁰ the larger λ_F in FeSe may result into enhanced quantum confinement effects. In single UC FeSe nanoflakes studied, therefore, as the nanoflake is reduced to nanoscale and comparable to λ_F (e.g. $A < \sim 150$ nm²), the lateral quantum confinement may become significant and result into a series of discrete energy levels, which will play a dominant role in Δ , with $k_F A^{0.5} \gg 1$ satisfied.¹⁰ Depending on A and positions, the number of these discrete energy levels within the pairing energy region around E_F may fluctuate and also be strongly enhanced, leading to substantial changes in Δ (even exceeding the bulk value Δ_0), as observed here. Such argument is also justified by observing the QSE-resulted fine peak structures beyond the E_F -near gap [Fig. 2(b)], which little take part in electron pairing and consequently superconductivity. Our study therefore provides the direct evidence of QSE in layered superconductor FeSe.

The occurrence of lateral QSE in single UC FeSe nanoflakes has been further solidified by taking STS on smaller nanoflakes, namely $A < 40$ nm², below which

Δ begins to increase in a prominent way. Figures 4(a) and 4(b) typify respectively the dI/dV spectra acquired on two FeSe nanoflakes with $A = 36$ nm² and $A = 27$ nm², both indicating significant electron-hole asymmetry in the peak strength (> 10). Furthermore, the gap magnitude Δ around E_F increases sharply with reducing A , regardless of position in a specific FeSe nanoflake. This contrasts sharply with Δ fluctuation around 17 meV for middle FeSe nanoflakes [Fig. 3(a)], and also the theoretically predicated reduction in superconducting gap Δ by QSE.^{9,10} All these results, together with the extremely large Δ (up to ~ 80 meV for the smaller A investigated) in Fig. 4(c), suggest that the gap observed here may be not related to superconductivity, and that the superconducting may be completely suppressed for small FeSe nanoflakes ($A < \sim 40$ nm²). Moreover, the differential conductance dI/dV spectra in Figs. 4(a) and 4(b) show a series of discrete energy levels both above and below E_F , which was never observed in FeSe films.¹⁴ The well defined energy peaks characterize the formation of quantum well states (QWS) due to the lateral QSE. Figure 4(c) plots the energy separation QWS between the highest occupied QWS and lowest unoccupied QWS as a function of A . Despite some scatter in the data, it is clear that Δ_{QWS} is anti-correlated with A , typical for QSE. More significantly, below the critical FeSe nanoflake area of ~ 40 nm², Δ_{QWS} appears larger than the gap magnitude in Fig. 2, leading to vanishing electron density of states (DOS) near E_F . Based on the Anderson criterion,²⁸ it will kill the superconductivity, which is in excellent agreement with our experiment.

Having demonstrated the dependence of spectroscopic characteristics on FeSe nanoflake area A , one may wonder whether the the asymmetric gap in Fig. 2 and discrete energy levels in Fig. 4 stem from the well-known Coulomb blockade (CB) in nanoscale tunnel junctions including STM technique.^{29–32} In CB effects, a series of pronounced peaks in dI/dV spectra with almost equal energy spacing are generated, which are little observed in middle-size FeSe nanoflakes [Fig. 2]. Moreover, if the CB effects are involved and take the sole responsibility for the gaps near E_F in Fig. 2, one should expect increasing average gap magnitude with reducing A . This contrasts with our observations where the average Δ remains nearly constant [Fig. 3(a)]. In Fig. 4, despite with several oscillations of dI/dV peaks for smaller FeSe nanoflakes, their separations are little equal. More significantly, we varied the tunneling separation and observed no dependence of the energies of dI/dV peaks. These observations consistently rule out the possibility that the CB effects taken the responsibility for the observed peaks in dI/dV spectra. Instead, we suggest that the asymmetric gaps in Fig. 2 may be superconductivity-related and the dI/dV peaks in Fig. 4 originate from QSE, as argued above.

We finally comment on the distinction of QSE observed here from those in Sn.¹⁰ Firstly, the gap magnitude Δ could be varied for a specific FeSe nanoflake [Fig. 2(b)], in sharp contrast to Sn nanoparticles.¹⁰ One possible rea-

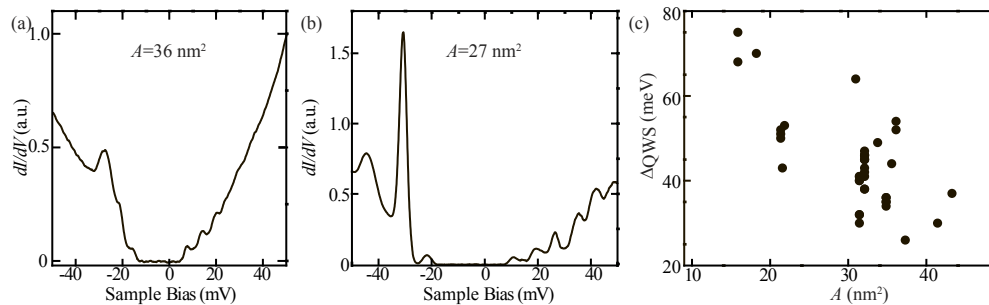


FIG. 4. (Color online) (a, b) dI/dV spectra on extremely small FeSe nanoflakes ($A < 40 \text{ nm}^2$), which shows distinct difference from those in larger FeSe nanoflakes ($A > 40 \text{ nm}^2$). (c) Plot of HOQWS-LUQWS separation Δ_{QWS} as function of FeSe nanoflake area A .

son may stem from the difference in the superconducting coherence length ξ . In Sn, $\xi \sim 240 \text{ nm}$ is considerably larger than the size of the studied nanoparticles,³³ from which Δ should change little with positions in a specific particle. However, ξ was found to be only 5.5 nm in thick FeSe films³⁴ and even smaller for single UC FeSe films due to the dimensionality effect. This appears smaller than the average lateral nanoflake size $A^{0.5}$ in Figs. 2 and 3. Therefore, the superconducting pairing, which depends on the local ($\sim \xi$) DOS, may alter with position in terms of possible variations in the local electron DOS. As a consequence, the superconductivity or gap magnitude Δ is expected to be site-dependent. In addition, a recent theoretical study has demonstrated that the superconducting order parameter or pairing could be varied with position by an order of magnitude if the nanograins is highly symmetric.³⁵ This provides an alternative explanation of the observed gap inhomogeneity in FeSe nanoflakes, which does appear quite symmetric [Fig. 1(a)] in shape as compared to the Sn nanoparticles.¹⁰ Secondly, the two coherence peaks in FeSe nanoflakes are asymmetric with respect to E_{F} [Fig. 3(b)], quite unexpected and distinct from the symmetric gaps in Sn nanoparticles as well.

Further experimental and theoretical investigations are needed to fully understand this intriguing phenomena.

IV. SUMMARY

In summary, our detailed STM/STS study has revealed the QSE in MBE-grown FeSe nanoflakes on SrTiO_3 substrate. The superconductivity-related gap magnitude Δ could be varied and reaches a value of $\sim 25 \text{ meV}$ as the area of FeSe nanoflakes ranges from $\sim 40 \text{ nm}^2$ to $\sim 150 \text{ nm}^2$. As A is further reduced, the superconductivity is completely suppressed due to strong QSE. The present study opens up the way to exploit the QSE on complex and layered unconventional superconductors.

ACKNOWLEDGMENTS

We thank T. Xiang for helpful conversations. This work was supported by National Science Foundation and Ministry of Science and Technology of China. All STM images were processed by Nanotec WSxM software.³⁶

* clsong07@gmail.com

† xucunma@mail.tsinghua.edu.cn

¹ Y. Guo, Y. F. Zhang, X. Y. Bao, T. Z. Han, Z. Tang, L. X. Zhang, W. G. Zhu, E. G. Wang, Q. Niu, Z. Q. Qiu, J. F. Jia, Z. X. Zhao, and Q. K. Xue, *Science* **306**, 1915 (2004).

² S. Y. Qin, J. Kim, Q. Niu, and C.-K. Shih, *Science* **324**, 1314 (2009).

³ T. Zhang, P. Cheng, W. J. Li, Y. J. Sun, G. Wang, X. G. Zhu, K. He, L. Wang, X. C. Ma, X. Chen, Y. Y. Wang, Y. Liu, H. Lin, J. F. Jia, and Q. K. Xue, *Nat. Phys.* **6**, 104 (2010).

⁴ A. Bezryadin, C. N. Lau, and M. Tinkham, *Nature* **404**, 971 (2000).

⁵ I. Giaever and H. R. Zeller, *Phys. Rev. Lett.* **20**, 1504 (1968).

⁶ D. C. Ralph, C. T. Black, and M. Tinkham, *Phys. Rev. Lett.* **74**, 3241 (1995).

⁷ J. von Delft, A. D. Zaikin, D. S. Golubev, and W. Tichy, *Phys. Rev. Lett.* **77**, 3189 (1996).

⁸ A. A. Shanenko, M. D. Croitoru, M. Zgirski, F. M. Peeters, and K. Arutyunov, *Phys. Rev. B* **74**, 052502 (2006).

⁹ A. M. García-García, J. D. Urbina, E. A. Yuzbashyan, K. Richter, and B. L. Altshuler, *Phys. Rev. Lett.* **100**, 187001 (2008).

¹⁰ S. Bose, A. M. García-García, M. M. Ugeda, J. D. Urbina, C. H. Michaelis, I. Brihuega, and K. Kern, *Nat. Mater.* **9**, 550 (2010).

¹¹ D. V. Averin and Y. V. Nazarov, *Phys. Rev. Lett.* **69**, 1993 (1992).

¹² A. M. García-García, J. D. Urbina, E. A. Yuzbashyan, K. Richter, and B. L. Altshuler, *Phys. Rev. Lett.* **100**, 187001 (2008).

¹³ H. Olofsson, S. Åberg, and P. Leboeuf, *Phys. Rev. Lett.* **100**, 037005 (2008).

- ¹⁴ Q. Y. Wang, Z. Li, W. H. Zhang, Z. C. Zhang, J. S. Zhang, W. Li, H. Ding, Y. B. Ou, P. Deng, K. Chang, J. Wen, C. L. Song, K. He, J. F. Jia, S. H. Ji, Y. Y. Wang, L. L. Wang, X. Chen, X. C. Ma, and Q. K. Xue, *Chin. Phys. Lett.* **29**, 037402 (2012).
- ¹⁵ W. H. Zhang, Y. Sun, J. S. Zhang, F. S. Li, M. H. Guo, Y. F. Zhao, H. M. Zhang, J. P. Peng, Y. Xing, W. H. Chao, T. Fujita, A. Hirata, Z. Li, H. Ding, C. J. Tang, M. Wang, Q. Y. Wang, K. He, S. Ji, X. Chen, J. F. Wang, Z. C. Xia, L. Li, Y. Y. Wang, J. Wang, L. Wang, M. W. Chen, Q. K. Xue, and X. C. Ma, *Chin. Phys. Lett.* **31**, 017401 (2014).
- ¹⁶ W. H. Zhang, Z. Li, F. S. Li, H. M. Zhang, J. P. Peng, C. J. Tang, Q. Y. Wang, K. He, X. Chen, L. Wang, X. C. Ma, and Q. K. Xue, *Phys. Rev. B* **89**, 060506 (2014).
- ¹⁷ D. F. Liu, W. H. Zhang, D. X. Mou, J. F. He, Y. B. Ou, Q. Y. Wang, Z. Li, L. Wang, L. Zhao, S. L. He, Y. Y. Peng, X. Liu, C. Y. Chen, L. Yu, G. D. Liu, X. L. Dong, J. Zhang, C. T. Chen, Z. Y. Xu, J. P. Hu, X. Chen, X. C. Ma, Q. K. Xue, and X. J. Zhou, *Nat. Commun.* **3**, 931 (2012).
- ¹⁸ S. L. He, J. F. He, W. H. Zhang, L. Zhao, D. F. Liu, X. Liu, D. X. Mou, Y. B. Ou, Q. Y. Wang, Z. Li, L. L. Wang, Y. Y. Peng, Y. Liu, C. Y. Chen, L. Yu, G. D. Liu, X. L. Dong, J. Zhang, C. T. Chen, Z. Y. Xu, X. Chen, X. C. Ma, Q. K. Xue, and X. J. Zhou, *Nat. Mater.* **12**, 605 (2013).
- ¹⁹ S. Y. Tan, Y. Zhang, M. Xia, Z. Ye, F. Chen, X. Xie, R. Peng, D. F. Xu, Q. Fan, H. C. Xu, J. Jiang, T. Zhang, X. C. Lai, T. Xiang, J. P. Hu, N. P. Xie, and D. L. Feng, *Nat. Mater.* **12**, 634 (2013).
- ²⁰ J. Bang, Z. Li, Y. Y. Sun, A. Samanta, Y. Y. Zhang, W. H. Zhang, L. Wang, X. Chen, X. C. Ma, Q. K. Xue, and S. B. Zhang, *Phys. Rev. B* **87**, 220503 (2013).
- ²¹ R. Peng, X. P. Shen, X. Xie, H. C. Xu, S. Y. Tan, M. Xia, T. Zhang, H. Y. Cao, X. G. Gong, J. P. Hu, B. P. Xie, and D. L. Feng, *Phys. Rev. Lett.* **112**, 107001 (2014).
- ²² J. F. Ge, Z. L. Liu, C. Liu, C. L. Gao, D. Qian, Q. K. Xue, Y. Liu, and J. F. Jia, *Nat. Mater.* Published online: 10.1038/nmat4153 (2014).
- ²³ M. Araújo, A. M. García-García, and P. D. Sacramento, *Phys. Rev. B* **84**, 172502 (2011).
- ²⁴ S. Mishra, K. Song, J. A. Koza, and M. Nath, *ACS Nano* **7**, 1145 (2013).
- ²⁵ S. Mishra, K. Song, K. C. Ghosh, and M. Nath, *ACS Nano* **8**, 2077 (2014).
- ²⁶ C. L. Song, Y. L. Wang, Y. P. Jiang, Z. Li, L. Wang, K. He, X. Chen, X. C. Ma, and Q. K. Xue, *Phys. Rev. B* **84**, 020503 (2011).
- ²⁷ Z. Li, J. P. Peng, H. M. Zhang, W. H. Zhang, H. Ding, P. Deng, K. Chang, C.-L. Song, S. H. Ji, L. Wang, K. He, X. Chen, Q. K. Xue, and X. C. Ma, *J. Phys.: Condens. Matter* **26**, 265002 (2014).
- ²⁸ P. W. Anderson, *J. Phys. Chem. Solids* **11**, 26 (1959).
- ²⁹ P. J. M. van Bentum, R. T. M. Smokers, and H. van Kempen, *Phys. Rev. Lett.* **60**, 2543 (1988).
- ³⁰ M. Amman, R. Wilkins, E. Ben-Jacob, P. D. Maker, and R. C. Jaklevic, *Phys. Rev. B* **43**, 1146 (1991).
- ³¹ M. Amman, S. B. Field, and R. C. Jaklevic, *Phys. Rev. B* **48**, 12104 (1993).
- ³² Z. F. Zhong, H. L. Shen, R. X. Cao, L. Sun, K. P. Li, J. Hu, Z. Liu, D. Wu, X. R. Wang, and H. F. Ding, *Phys. Rev. B* **88**, 125408 (2013).
- ³³ C. Kittel and P. McEuen, *Introduction to solid state physics*, Vol. 8 (Wiley New York, 1976).
- ³⁴ C. L. Song, Y. L. Wang, Y. P. Jiang, L. Wang, K. He, X. Chen, J. E. Hoffman, X. C. Ma, and Q. K. Xue, *Phys. Rev. Lett.* **109**, 137004 (2012).
- ³⁵ M. Croitoru, A. A. Shanenko, C. C. Kaun, and F. M. Peeters, *Phys. Rev. B* **83**, 214509 (2011).
- ³⁶ I. Horcas, R. Fernandez, J. M. Gomez-Rodriguez, J. Colchero, J. Gómez-Herrero, and A. M. Baro, *Rev. Sci. Instru.* **78**, 013705 (2007).